

# Nanoscale

Accepted Manuscript



This is an *Accepted Manuscript*, which has been through the Royal Society of Chemistry peer review process and has been accepted for publication.

*Accepted Manuscripts* are published online shortly after acceptance, before technical editing, formatting and proof reading. Using this free service, authors can make their results available to the community, in citable form, before we publish the edited article. We will replace this *Accepted Manuscript* with the edited and formatted *Advance Article* as soon as it is available.

You can find more information about *Accepted Manuscripts* in the [Information for Authors](#).

Please note that technical editing may introduce minor changes to the text and/or graphics, which may alter content. The journal's standard [Terms & Conditions](#) and the [Ethical guidelines](#) still apply. In no event shall the Royal Society of Chemistry be held responsible for any errors or omissions in this *Accepted Manuscript* or any consequences arising from the use of any information it contains.



## Nanoscale

## PAPER

## Fabrication of biofuel cell improved by $\pi$ -conjugated electron pathway effect induced from a new enzyme catalyst employing terephthalaldehyde

Received 00th January 20xx,  
Accepted 00th January 20xx

DOI: 10.1039/x0xx00000x

[www.rsc.org/nanoscale](http://www.rsc.org/nanoscale)

Yongjin Chung, Kyu Hwan Hyun, and Yongchai Kwon\*

A model explaining  $\pi$ -conjugated electron pathway effect induced from a novel cross linker-adopted enzyme catalyst is suggested and performance and stability of enzymatic biofuel cell (EBC) adopting the new catalyst are evaluated. For the purpose, new terephthalaldehyde (TPA) and conventional glutaraldehyde (GA) cross-linkers are adopted on glucose oxidase (GOx), polyethyleneimine (PEI) and carbon nanotube (CNT) (GOx/PEI/CNT) structure. GOx/PEI/CNT cross-linked by TPA (TPA/[GOx/PEI/CNT]) results in superior EBC performance and stability to other catalysts. It is attributed to  $\pi$  bonds conjugated between aldehyde of TPA and amine of GOx/PEI molecules. By the  $\pi$  conjugation, electrons bonded with carbon and nitrogen are delocalized, promoting electron transfer and catalytic activity with excellent EBC performance. Maximum power density (MPD) of EBC adopting the TPA/[GOx/PEI/CNT] ( $0.66 \text{ mWcm}^{-2}$ ) is far better than that of other EBCs (MPD of EBC adopting GOx/PEI/CNT is  $0.40 \text{ mWcm}^{-2}$ ). Regarding stability, covalent bonding formed between TPA and GOx/PEI plays a critical role in preventing denaturation of GOx molecules, leading to excellent stability. By the repeated measurements of catalytic activity, TPA/[GOx/PEI/CNT] maintain its activity to 92% of its initial value even after five weeks.

### 1. Introduction

As demands about eco-friendly energy production are getting increased due to depletion of conventional fossil fuels and pollution occurring via excessive utilization of the fossil fuels, associated research including enzymatic biofuel cell (EBC) that can convert the eco-friendly bioenergy extracted from biomass into the electrical energy have been considered desirable alternative.<sup>1-6</sup> Of the EBCs, one adopting glucose oxidase (GOx) as the biocatalyst has recently emerged due to the following reasons. First, its electromotive force (EMF) of EBC employing GOx is relatively high ( $\sim 1 \text{ V}$  at physiological pH) among the EBC systems operated by using biocatalysts.<sup>7,8</sup> Second, EBC process using GOx and glucose as biocatalyst and fuel is simpler and easier than alcohol based biofuel cells because it doesn't need to additional step to extract alcohols from natural resources like sugarcane. Third, the GOx-based EBC can be served as semi-permanent cardiac pacemakers and micro medical devices because it has strong compatibility and specification with human body in that glucose and oxygen contained in human blood are consumed.<sup>2,7</sup>

However, notwithstanding such positive aspects of EBC system, commercialization of the EBC has still a long way to go due to low EBC performance and its short lifetime. The drawbacks are attributed to low loading of enzyme clusters, slow charge transfer rate and poor catalytic activity of enzyme. Ultimately, poor enzyme immobilization is a main reason for the problems.

To date, to overcome the difficulties, a myriad of methods have been developed. Particularly, (i) physical adsorptions like non-covalent adsorption and physical entrapment and (ii) chemical bonding like encapsulation, covalent coupling, affinity bonding and enzyme cross-linking have been mainly attempted even though appropriate enzyme immobilization procedure have not been determined yet.<sup>2,9-12</sup>

As an alternative way to enhance the EBC performance and stability, polymerizing GOx molecules by cross-linker such as glutaraldehyde (GA) has been suggested due to cheap cost, easy treatment and high possibility of direct bonding with GOx molecules. The GOx molecules are usually polymerized by aldol condensation occurring between cross-linkers of GA and free amino groups of GOx. However, the use of GA is prone to retard mass transfer of glucose molecules to active sites of GOx due to blockage of the GOx active sites that are covered by GA. Namely, GA can prevent electron transfer between active sites of GOx and outer part of GOx.<sup>13,14</sup>

Graduate school of Energy and Environment, Seoul National University of Science and Technology, 232Gongneung-ro, Nowon-gu, Seoul, 139-743, Republic of Korea. E-mail: [kwony@seoultech.ac.kr](mailto:kwony@seoultech.ac.kr); Tel: +82-29706805, +82-29706800

† Footnotes relating to the title and/or authors should appear here.

Electronic Supplementary Information (ESI) available: [details of any supplementary information available should be included here]. See DOI: 10.1039/x0xx00000x

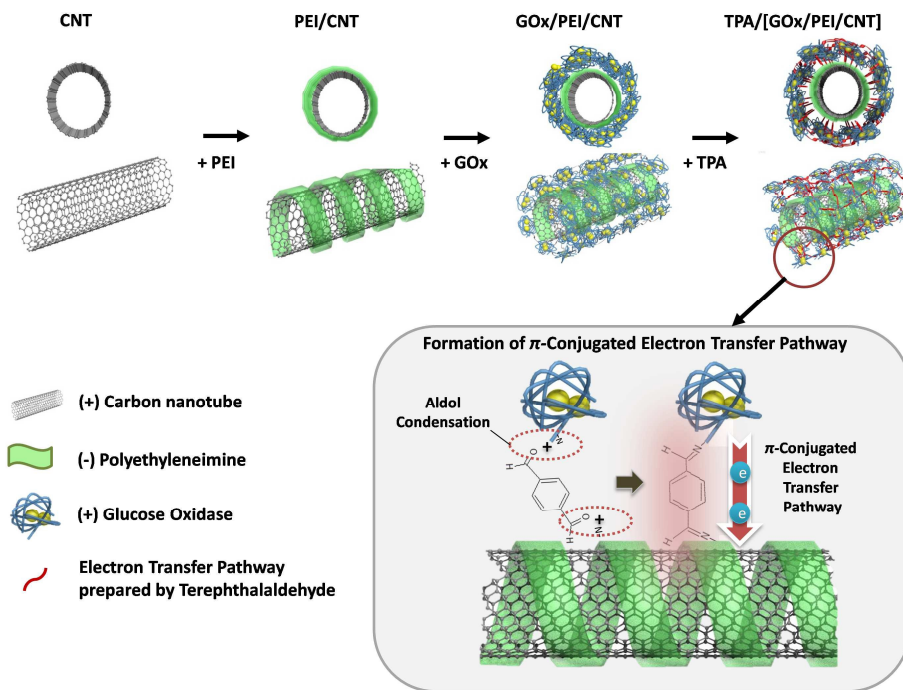


Fig. 1 Schematic illustrations showing the fabrication of the catalysts.

To alleviate the issues of GA, in this study, we use terephthalaldehyde (TPA) as a new cross-linking coupling agent. According to our results, when TPA is used as the cross-linker, the mass transfer retardation problem that is a major drawback of GA is considerably reduced. For use of the TPA, first, GOx molecules are physically entrapped on the structure consisting of polyethyleneimine (PEI) and carbon nanotube (CNT) substrate. In turn, TPA is provided as a coupling agent for polymerizing the GOx and PEI. Through the process, both GOx-PEI and GOx-GOx molecules create  $\pi$  conjugated bonds that play a role as pathway to promote electron transfer.

Here, PEI is a conductive polymer (CP) and acted as a pathway for facilitating electron transfer from flavin adenine dinucleotide (FAD) within GOx molecules to CNT substrate. In addition, since the PEI is positively charged and GOx is negatively charged in neutral condition, the GOx molecules are entrapped by the PEI molecules through attractive force. Also, unlike other major CPs like poly(dimethyl diallylammonium chloride) (PDDA) and polyaniline (PANI), since the PEI has abundant free amino groups, it can form more covalent bonds with amino groups of GOx.<sup>15,16</sup>

TPA is a cross-linking coupling agent and its terminal parts consist of aldehyde groups. Due to that, covalent bonding between free amino groups of GOx and PEI occurs. As a result of that, N=C bonds are formed. However, unlike GA, the N=C bonds of TPA are resonated with N-C bonds due to  $\pi$ -conjugation with phenyl group, inducing faster movement of

electrons than GA-bonded GOx/PEI/CNT layer. To evaluate the above proposed  $\pi$ -conjugation effect on EBC performance and stability, differences in chemical structure of GOx/PEI/CNT layer bonded by TPA and GA are measured by Fourier Transport Infrared (FTIR) spectrometer. Cyclic voltammogram (CV) is also used to demonstrate electron transfer mechanism. Based on the evaluations, we expect that our research result will be the milestone to consolidate a baseline protocol of enzyme immobilized catalyst structure.

## 2. Experimental

### 2.1 Chemicals

Multiwall carbon nanotubes (MWCNT), with ~95% purity, were obtained from NanoLab (Brighton, MA). polyethyleneimine (PEI) (50wt% solution in water, MW 750,000), glutaraldehyde (GA) (25% solution in water), terephthalaldehyde (TPA) 99%, glucose oxidase (GOx, from *Aspergillus niger* type XeS, 100,000 unit/g solid) and b-D-glucose were purchased from Sigma-Aldrich (Milwaukee, WI, USA).

### 2.2 Fabrication and characterizations of catalysts

GOx/PEI/CNT layer was fabricated by stepwise deposition of positively charged PEI and negatively charged GOx on

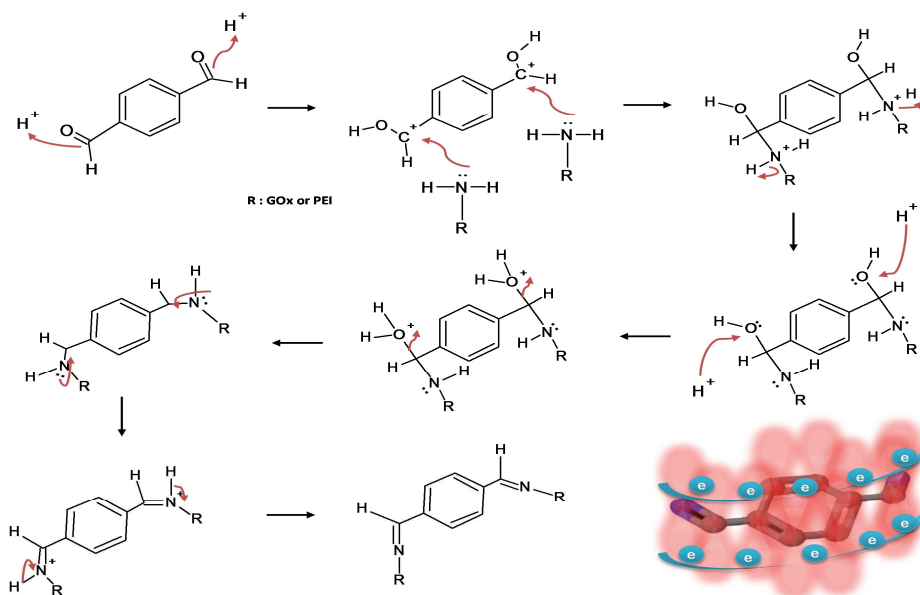


Fig. 2 The reaction mechanism occurring between aldehyde group of TPA and lysine residue of GOx and PEI.

MWCNT, meaning that the GOx/PEI/CNT layer is physically bonded with relatively weak bonding force. As the synthetic procedure, PEI was initially adsorbed onto CNT by dissolving 20 mg of MWCNTs into 10 mL of PEI solution that was diluted with deionized (DI) water until its concentration reached  $2.5 \text{ mg}\cdot\text{mL}^{-1}$ , and the mixture underwent sonication for 10 min and was stirred for 1 h. Excessive PEI was removed by washing using DI water. Then, the PEI/CNT was immersed in GOx solution ( $2.0 \text{ mg}\cdot\text{mL}^{-1}$  in  $0.1 \text{ mM}$  PBS) for 20 min, completing GOx/PEI/CNT layer. In order to form cross-linked GOx/PEI/CNT layer, the GOx/PEI/CNT layer was immersed in GA ( $0.5\%$  (w/v) in DI water) or TPA ( $0.5\%$  (w/v) in ethanol) for 2 h. The schematic illustration depicting synthetic procedure of GOx/PEI/CNT layers cross-linked by TPA or GA is shown in Fig. 1. Electrochemical characterizations of the catalysts were explained in supplementary information (SI) section.<sup>17-19</sup>

### 3. Results and discussion

#### 3.1 Evaluation of Chemical Structure

It is critical to investigate how GA and TPA affect electron transfer occurring in GOx/PEI/CNT, followed by performance and stability of EBC because (i) there is a disparity in reaction mechanism between the two different cross-linkers (GA and TPA) and GOx/PEI/CNT and (ii) it is not sure yet whether which mechanism is more effective to improve the performance and stability of EBC. When GA or TPA is provided to crosslink the GOx/PEI/CNT, lysine residue of GOx and free amine group of

PEI are reacted with aldehyde group of GA or TPA by aldol condensation. With that, chemical bonding consisting of strong covalent bonds between C and N are formed at both ends of the cross-linkers. Namely, with adoption of the cross-linkers, strong chemical bonding is configured between GOx and cross-linker and between PEI and cross-linker, although relatively weak physical bonding is formed inside GOx/PEI/CNT.

Because chemical bonding may lead to (i) strong bonding amid the GOx, PEI and cross-linker and (ii) distance less than 2 nm between GOx and PEI that is required for direct electron transfer,<sup>20-23</sup> use of the cross-linkers can result in stable GOx/PEI/CNT and fast electron transfer.

More specifically, the electron transfer is more promoted in enzyme structure including TPA than that including GA due to electron transfer facilitated by the formation of  $\pi$ -conjugated bonds. According to Fig. 2, when GA is employed, N=C bonds formed at the both ends (GOx-GA and GA-PEI) are not properly served as electron transfer pathway in overall structure of N=C-aliphatic-C=N because conductivity of the aliphatic and its adjacent bonds are poor. Also, the N=C bonds are rigidly stuck together and it is therefore difficult for electrons to move fast via the strictly bonded N=C bonds. In contrast, with utilization of TPA, N=C-phenyl-C=N structure that includes  $\pi$ -conjugated bonds are produced amid GOx, PEI and TPA. As explained in Figs. 1 and 2, the bonds occurring between C and N of the enzyme structure are conjugated with adjacent phenyl group, resonating as single and double bonds depending on under the given condition. Alternation of the electron configurations induces fast electron movement, facilitating electron transfer and reaction rate. The positive

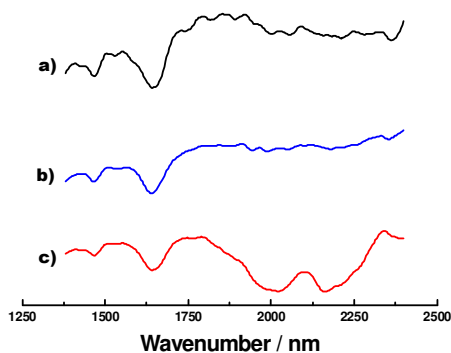


Fig. 3 FTIR spectra of a) GOx/PEI/CNT, b) GA/[GOx/PEI/CNT] and c) TPA/[GOx/PEI/CNT] structures.

impact of  $\pi$ -conjugated bond on electron transfer was already reported by other references.<sup>24-27</sup>

To check out whether bond formations hypothesized in Fig. 2 are appropriate, FTIR measurements are performed using GOx/PEI/CNT structure that are cross-linked with GA and TPA (GA/[GOx/PEI/CNT] and TPA/[GOx/PEI/CNT]) and a structure without the cross-linking agent (GOx/PEI/CNT). The result is presented in Fig. 3. In the FTIR data, only TPA/[GOx/PEI/CNT] showed peaks at 1800~2080 and 2120~2240 nm.<sup>28-30</sup> Appearance of the peaks is due to conjugated N=C bonds that were associated with adjacent phenyl groups. According to Kristen *et al.*,<sup>31</sup> single bond conjugations of N=C bonds were appeared at near 1960 nm, while its double bonds were observed at 2170 nm. It was well matched with the peak ranges observed at TPA/[GOx/PEI/CNT].

Unlike TPA/[GOx/PEI/CNT], there were no peaks in GA/[GOx/PEI/CNT] showing  $\pi$ -conjugated electron transfer pathway, indicating the structure had little further electron transfer pathway induced by  $\pi$ -conjugated bonds and slow reaction rate compared to TPA/[GOx/PEI/CNT].

### 3.2 Electrochemical evaluations of enzyme structure bonded with different cross-linkers

Based on the FTIR results, it is required to investigate trend in both active surface area and redox reaction of FADs within GOx(GOx(FAD) + 2H<sup>+</sup> + 2e<sup>-</sup> ↔ GOx(FADH<sub>2</sub>)) in the corresponding enzyme structures. First, roles of PEI and GOx were evaluated by CV measurements (Fig. 4). In the Fig. 4a, there were no peaks in GCE and PEI/CNT/GCE, whereas a clear redox peak was observed in GOx/PEI/CNT/GCE, proving that redox reaction of FAD took place in structure including GOx. When it came to envelope current, use of CNT and PEI promoted its increment.

To inspect the effect of cross-linker on catalytic activity of GOx/PEI/CNT, related CV curves were measured and compared (Fig. 4b). According to the Fig. 4b, FAD redox reaction peak of TPA/[GOx/PEI/CNT]/GCE was higher than that of GA/[GOx/PEI/CNT]/GCE, while the peak in GOx/PEI/CNT/GCE and GA/[GOx/PEI/CNT]/GCE was similar together. It means that  $\pi$ -conjugated bonds formed by crosslinking between TPA and GOx/PEI facilitate transfer of electrons generated/consumed by redox reaction of FADs, while N=C bonds formed between GA and GOx/PEI did not work effectively for both electron transfer and redox reaction of FADs. Indeed, these results were compatible with FTIR result. As next step, what is rate determining step of the corresponding structures is evaluated (Fig. 5). In all CV curves, peak currents for the FAD redox reaction were linearly increased to potential scan rate, confirming that the three different structures were controlled by a surface reaction.

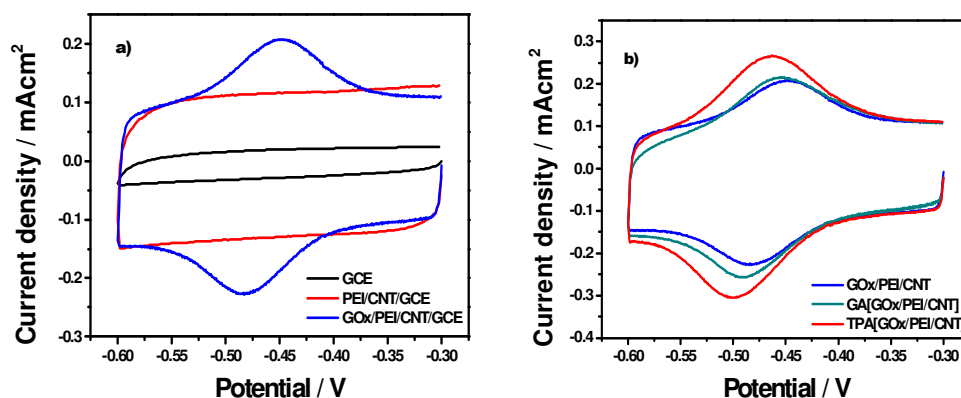
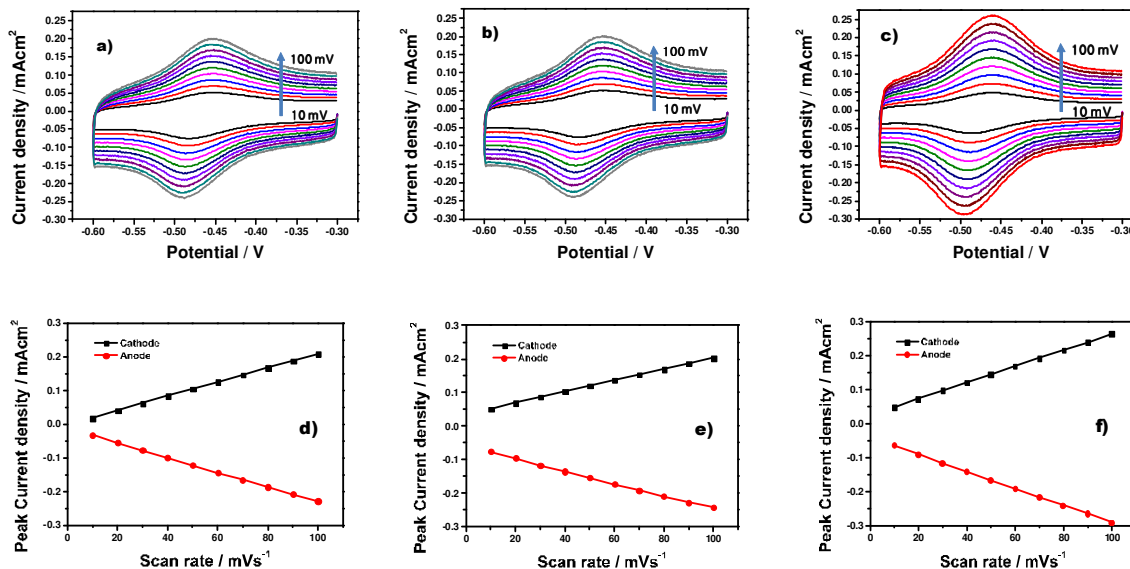


Fig. 4 Cyclic Voltammograms of a) GCE, PEI/CNT/GCE, GOx/PEI/CNT/GCE and b) GOx/PEI/CNT/GCE, GA/[GOx/PEI/CNT] and TPA/[GOx/PEI/CNT]. For CV tests, 0.01M PBS(pH 7.4) was used as an electrolyte at N<sub>2</sub> state and potential scan rate was 100mV s<sup>-1</sup>.



**Fig. 5** Cyclic voltammograms of a) GOx/PEI/CNT, b) GA/[GOx/PEI/CNT], c) TPA/[GOx/PEI/CNT] and a plot between peak current density and scan rate of d) GOx/PEI/CNT, e) GA/[GOx/PEI/CNT], f) TPA/[GOx/PEI/CNT]. For the CV tests, 0.01 M PBS (pH 7.4) was used as an electrolyte at N<sub>2</sub> state, while potential scan rate was ranged from 10 to 100 mV s<sup>-1</sup>.

Furthermore, the differences in peak potential,  $\Delta E_p$  of GOx/PEI/CNT, GA/[GOx/PEI/CNT] and TPA/[GOx/PEI/CNT] were 37, 40 and 32 mV at a scan rate of 100 mV s<sup>-1</sup>, demonstrating that they were within quasi-reversible reaction region.<sup>32-33</sup> The formal potential calculated at GOx/PEI/CNT, GA/[GOx/PEI/CNT] and TPA/[GOx/PEI/CNT] is -0.465, -0.465, -0.476 V vs. Ag/AgCl and they were similar to the standard potential for FAD redox reaction (-0.486 V at pH 7.4), implying that they were served as the catalyst for FAD redox reaction.<sup>33</sup> Meanwhile, in comparison of the three structures,  $\Delta E_p$  of TPA/[GOx/PEI/CNT] was smallest, while its formal potential was the closest to standard potential for FAD redox reaction. Taken together, it is

summarized that TPA/[GOx/PEI/CNT] is the best catalyst for facilitating FAD redox reaction.

Gaining electron transfer rate constant ( $k_s$ ) value is useful because electron transfer rate affecting EBC performance is proportional to the  $k_s$ . For getting the value, Laviron's formula was adopted and the results are represented in Fig. 6.<sup>34</sup>  $k_s$ s of GOx/PEI/CNT, GA/[GOx/PEI/CNT] and TPA/[GOx/PEI/CNT] were 5.23, 5.68 and 5.81 s<sup>-1</sup>, indicating that electron transfer rate constant of TPA/[GOx/PEI/CNT] was highest due to  $\pi$  conjugation effect. Also, these  $k_s$ s were better than that of other similarly formed enzyme structures. For instance, the value in the GOx/PEI/carbon paper was 2.3 s<sup>-1</sup>,<sup>32</sup> that in

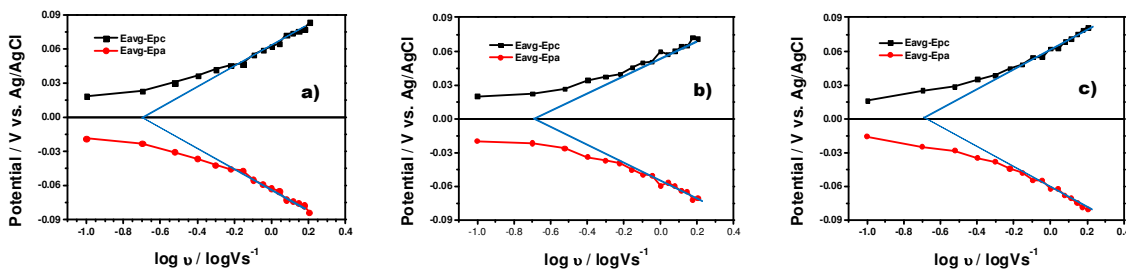


**Fig. 6** Laviron's plot of a) GOx/PEI/CNT, b) GA/[GOx/PEI/CNT], c) TPA/[GOx/PEI/CNT]. For the CV tests, 0.01 M PBS (pH 7.4) was used as an electrolyte at N<sub>2</sub> state, while potential scan rate was ranged from 100 to 1600 mV s<sup>-1</sup>.



GA/[GOx/gelatin/CNT] structure was  $1.08 \text{ s}^{-1}$ ,<sup>35</sup> that in the GOx/CNT structure was  $2.9 \text{ s}^{-1}$ .<sup>36</sup>

To elucidate mechanism of oxidation reaction occurring at anode electrode of EBC that has been known as rate determining reaction determining EBC performance, it could not be better than evaluating the effect of oxygen mediator ( $\text{O}_2$  mediator) on catalytic activity of the structures. Air state (with  $\text{O}_2$ ) and  $\text{N}_2$  state (without  $\text{O}_2$ ) were used for that, while glucose was optionally supplied.

Fig.S1 represents CV curves of the structures operated at "without  $\text{O}_2$ " condition ( $\text{N}_2$  state) and "with  $\text{O}_2$ " condition (air state) without glucose. In air state, CV curves were shifted to downward with the redox peak appeared around  $-0.45 \text{ V}$  vs. Ag/AgCl. The downward shift of the CV curves is due to  $\text{O}_2$  reduction reaction ( $\text{O}_2 + 2\text{H}^+ + 2\text{e}^- \rightarrow \text{H}_2\text{O}_2$ ). Similar result was already reported.<sup>1,19,37</sup>

Fig.S2 shows CV curves presenting how glucose affects catalytic activity at  $\text{N}_2$  state. For the tests, 10mM glucose was supplied. The CV curves measured remained unchanged irrespective of provision of glucose, demonstrating that glucose did not have an influence on redox reaction of FAD. It indicates that a mediator is required to link both oxidation

reaction of glucose and redox reaction of FAD.<sup>1,37,38</sup>

For the purpose of comparison with Fig. 4, CV curves presenting how glucose affects catalytic activity at air state were measured and the result is represented in Fig.7. Here, 0.1 ~ 10 mM glucose was provided. According to the Fig.7, three unique experimental observations were found.

First, as glucose concentration increased, reduction current peak rapidly dropped. It is due to prohibition in reduction reaction of FAD. Namely, with supply of glucose, glucose oxidation reaction ( $\text{Glucose} \rightarrow 2\text{H}^+ + 2\text{e}^- + \text{Gluconolactone}$ ) occurs. Electrons and protons generated by the glucose oxidation reaction are then provided for reduction reaction of FAD and thereby, current peak for the reduction reaction of FAD ( $\text{GOx (FAD)} + 2\text{H}^+ + 2\text{e}^- \rightarrow \text{GOx (FADH}_2\text{)}$ ) decreases.

Second, with oxidation reaction of FAD ( $\text{FADH}_2 \rightarrow \text{GOx (FAD)} + 2\text{H}^+ + 2\text{e}^-$ ), some electrons and protons generated are spent for reduction reaction of  $\text{O}_2$  ( $\text{O}_2 + 2\text{H}^+ + 2\text{e}^- \rightarrow \text{H}_2\text{O}_2$ ), inducing small drop in current peak for oxidation reaction of FAD that is appeared at  $-0.63 \text{ V}$  vs. Ag/AgCl. Based on the above two observations, it is concluded that  $\text{O}_2$  makes a bridge role in inducing electron transfer between FAD and glucose.

Third, reactivity for FAD redox reaction is the best in

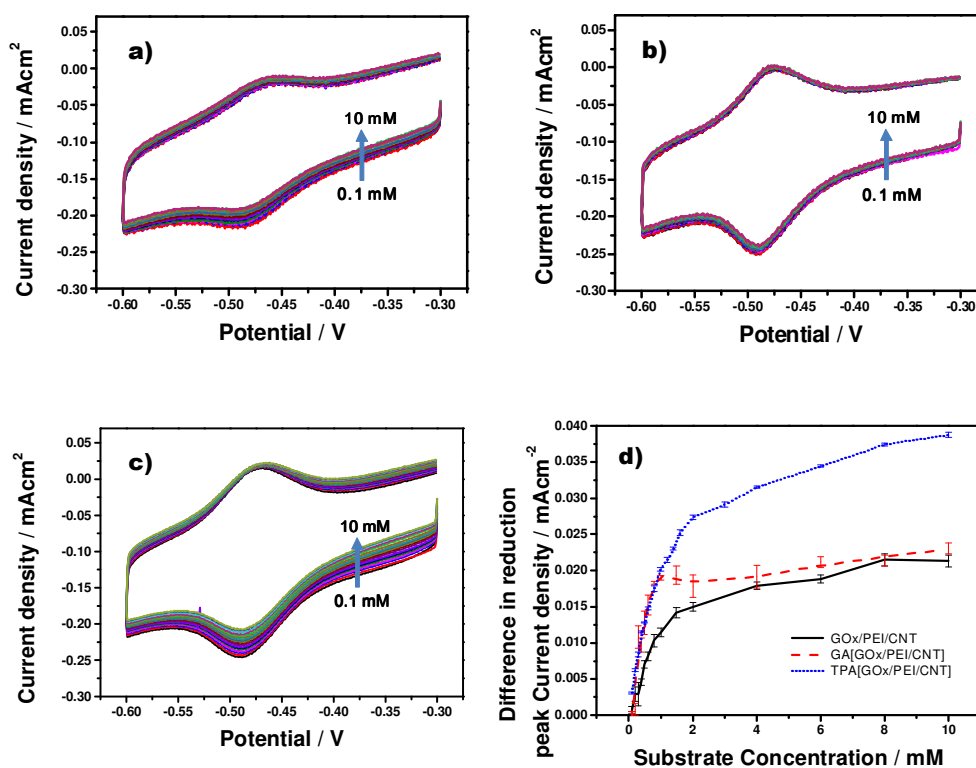


Fig. 7 Cyclic voltammograms of a) GOx/PEI/CNT, b) GA/[GOx/PEI/CNT], c) TPA/[GOx/PEI/CNT] run at air state with provision of 0.1~10mM glucose and d) a relationship between glucose concentration and difference in reduction peak current of FAD. For the CV tests, 1.0 M PBS (pH 7.4) was used as electrolyte and potential scan rate was  $50 \text{ mV s}^{-1}$ .

TPA/[GOx/PEI/CNT]. It is ascribed to promoted electron transfer pathway. Related to trend of the FAD redox reaction reactivity, change in peak current for reduction reaction of FAD is measured with stepwise increase in glucose concentration three times (see Fig.7d). According to the Fig.7d, in TPA/[GOx/PEI/CNT], the peak current was reproducibly obtained with a standard deviation (SD) of 0.248, while SDs of the value in GOx/PEI/CNT and GA/[GOx/PEI/CNT] were 0.713 and 1.456.

It means that the TPA/[GOx/PEI/CNT] is better catalyst than other ones for occurrence of pertinent FAD reaction. Meanwhile, based on the Fig.7d and Michaelis-Menten equation calculated from Lineweaver-burk plot,<sup>39,40</sup> maximum current density ( $J_{max}$ ) was gained. The values in GOx/PEI/CNT, GA/[GOx/PEI/CNT] and TPA/[GOx/PEI/CNT] were 24.4, 24.4 and 45.5  $\mu\text{A}\cdot\text{cm}^{-2}$ . Surprisingly,  $J_{max}$  in TPA/[GOx/PEI/CNT] was twice higher than that in others, while difference of the value in GA/[GOx/PEI/CNT] and GOx/PEI/CNT was trivial.

For inspecting whether the TPA/[GOx/PEI/CNT] induces desirable two-electron and two-proton redox reaction of FAD ( $\text{GOx}(\text{FAD}) + 2\text{H}^+ + 2\text{e}^- \leftrightarrow \text{GOx}(\text{FADH}_2)$ ), redox peak potential is recorded with increase in electrolyte pH (Fig.S3). As the electrolyte pH increased from 5.09 to 9.06, redox peak potential was linearly reduced with the slope of  $-52.7 \text{ mV pH}^{-1}$ , which was well agreed with theoretical value ( $-58.6 \text{ mV pH}^{-1}$ ),<sup>34,38</sup> Based on that, it is obvious when TPA/[GOx/PEI/CNT] is used, both redox reaction of FAD and glucose oxidation reaction are facilitated with excellent reproducibility.

### 3.3 Performance of EBCs adopting enzyme structures bonded with different cross-linkers

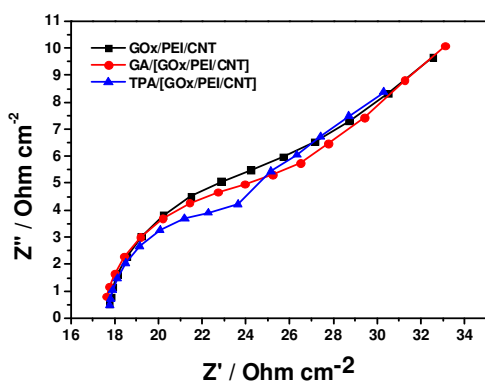


**Fig. 8** EIS measurements of EBCs adopting the biocatalysts as enzymatic anodic catalyst. In the tests, 0.2 M glucose solution was fed and circulated as a fuel from an external bottle to the anode chamber of the EBC at a rate of 60  $\text{mL min}^{-1}$ , while 20  $\text{cc min}^{-1}$  of  $\text{H}_2$  gas was fed to the cathode.

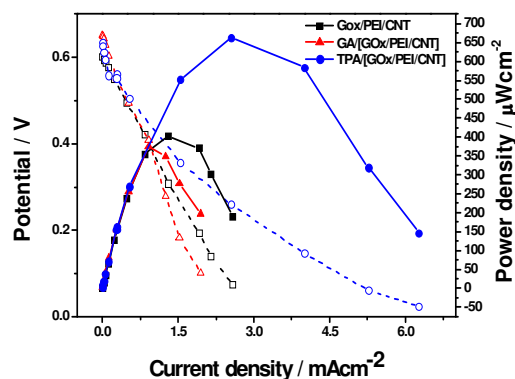


**Fig. 9** Polarization curves of EBCs adopting the biocatalysts as an enzymatic anodic catalyst and Pt as a cathodic catalyst. In the tests, 0.2 M glucose solution was fed and circulated as a fuel from an external bottle to the anode chamber of the EBC at a rate of 60  $\text{mL min}^{-1}$ , while 50  $\text{cc min}^{-1}$  of  $\text{O}_2$  gas was fed to the cathode.

Performances of EBCs adopting the three enzyme structures as catalyst of anode are investigated by the measurements of their polarization curves (Fig. 8) and EISs (Fig. 9). According to the Fig. 8, maximum power density (MPD) of EBC adopting TPA/[GOx/PEI/CNT] was twice better than that of EBCs adopting GA/[GOx/PEI/CNT] and GOx/PEI/CNT, while that of EBCs adopting GA/[GOx/PEI/CNT] and GOx/PEI/CNT was similar together (MPDs of EBCs adopting GOx/PEI/CNT, GA/[GOx/PEI/CNT] and TPA/[GOx/PEI/CNT] were 0.40, 0.37 and 0.66  $\text{mW}\cdot\text{cm}^{-2}$ ).

This result was well agreed with the data of Fig. 7d. Namely,  $J_{max}$  of TPA/[GOx/PEI/CNT] was twice better than that of GA/[GOx/PEI/CNT] and GOx/PEI/CNT, while  $J_{max}$  of GA/[GOx/PEI/CNT] and GOx/PEI/CNT was similar together. Since power density is theoretically proportional to current density, it is reasonable that a relationship between MPD (Fig. 8) and  $J_{max}$  (Fig. 7d) (the twice better result in both MPD and  $J_{max}$ ) is compatible.

To verify the correlation between EBC performance and catalytic activity, EISs were also measured and  $R_{ct}$ s and  $R_s$ s of the EBCs used for Fig. 8 were calculated (Fig. 9). According to the Fig. 9, difference in  $R_s$  of the three EBCs was not significant ( $17.5 \sim 18.0 \Omega\cdot\text{cm}^2$ ). On the other hand, Regarding  $R_{ct}$  of EBCs, that adopting TPA/[GOx/PEI/CNT] was lowest ( $26.9 \Omega\cdot\text{cm}^2$ ), while that adopting GOx/PEI/CNT and GA/[GOx/PEI/CNT] were 28.5 and 29.2  $\Omega\cdot\text{cm}^2$ . It is explained that  $\pi$  conjugated bonds of TPA/[GOx/PEI/CNT] promote charge (electron) transfer by electron resonance effect, reducing resistance against the charge transfer. Eventually, such an enhancement in charge (electron) transfer might be one of reasons for better catalytic activity and EBC performance.



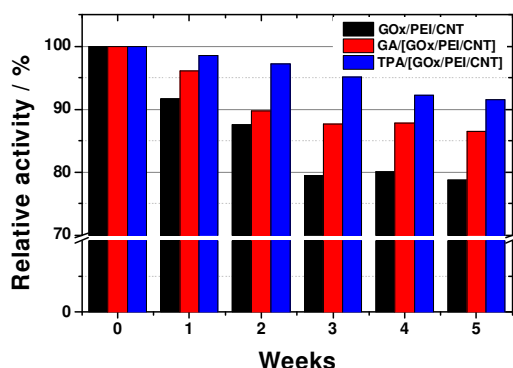


**Fig. 10** Stability measurements of the three layers estimated by regular measurement of their catalytic activity (FAD redox reaction peak) for five weeks.

It deserves to note that MPD of EBCs adopting the three enzyme structures is better than that of EBCs adopting other enzymatic catalyst structures. For instance, the MPD of cross-linked via GA cluster of GOx/CNT with benzoquinone mediator (Pt-C cathode) was  $0.12 \sim 0.37 \text{ mW}\cdot\text{cm}^{-2}$ ,<sup>41</sup> GOx/linear PEI/CNT was  $0.113 \text{ mW}\cdot\text{cm}^{-2}$  and Glucose dehydrogenase/linear PEI/CNT(laccase/CNT cathode) was  $0.513 \text{ mW}\cdot\text{cm}^{-2}$ .<sup>42</sup>

### 3.4 Stability of enzyme structures bonded with different cross-linkers

Stability of TPA/[GOx/PEI/CNT], GA/[GOx/PEI/CNT] and GOx/PEI/CNT structures is estimated by regular measurement of their catalytic activity (FAD redox reaction peak) for five weeks (Fig.10). According to the Fig.10, there are two main points to notify.

First, when catalytic activity of enzyme structures formed by cross-linkers (TPA/[GOx/PEI/CNT] and GA/[GOx/PEI/CNT]) was well maintained compared to that of GOx/PEI/CNT (after five weeks, GOx/PEI/CNT, GA/[GOx/PEI/CNT] and TPA/[GOx/PEI/CNT] maintained their catalytic activity to 78, 86 and 92 % of its initial value, respectively). This result is attributed to strong covalent bonding formed amid aldehyde group of the cross-linkers, lysine residue of GOx and free amine group of PEI. Namely, the C and N included in bonds formed between GA/TPA and GOx/PEI were served as adhesion promoter for strong immobilization of GOx on the substrate, thereby, denaturation of the GOx molecules was prevented and their catalytic activity was maintained.

Second, TPA/[GOx/PEI/CNT] was more stable than GA/[GOx/PEI/CNT]. It is explained that besides strong covalent bonding formed by amine,  $\pi$  conjugated bonds induced by TPA additionally affect strong immobilization of GOx molecules.

## 4. Conclusion

Performance and stability of enzymatic biofuel cell (EBC) adopting GOx/PEI/CNT based catalysts including cross-linkers like TPA and GA were investigated. After the related characterizations, GOx/PEI/CNT cross-linked by TPA (TPA/[GOx/PEI/CNT]) produced better EBC performance and stability than GA/[GOx/PEI/CNT] and GOx/PEI/CNT. It is ascribed to generation of  $\pi$  bonds conjugated between aldehyde groups of TPA and amine groups of GOx/PEI molecules. With the  $\pi$  conjugation, electrons belonging to N=C bonds are delocalized and such electron delocalization facilitates electron transfer and EBC performance, while the  $\pi$  conjugation was proved by FTIR measurements.

Effect of cross-linker on catalytic activity of GOx/PEI/CNT was evaluated by measurements of CV curves. According to the results, TPA/[GOx/PEI/CNT] induced the best FAD redox reaction, electron transfer rate,  $J_{\text{max}}$ . It turned out that the positive indices on catalytic activity gained in TPA/[GOx/PEI/CNT] were attributed to electron transfer pathway facilitated by the formation of  $\pi$ -conjugated bonds.

Regarding evaluation of EBC polarization curves that was a direct way to quantify EBC performance, MPD of EBC adopting TPA/[GOx/PEI/CNT] was two times better than that of other EBCs, confirming that the TPA/[GOx/PEI/CNT] resulted in high EBC performance.

Even in a prospect of stability, catalytic activity of TPA/[GOx/PEI/CNT] kept 92% of its initial value after five weeks, while TPA/[GOx/PEI/CNT] and GOx/PEI/CNT keep 86 and 78 % of their initial values after the period. It was because covalent bonding and  $\pi$  conjugation formed between TPA and GOx/PEI prevented denaturation of GOx molecules.

## Acknowledgements

This research was supported by Basic Science Research Program through the National Research Foundation of Korea (NRF) funded by the Ministry of Education (NRF-2013R1A1A2006494).

## References

- 1 K. H. Hyun, S. W. Han, W.-G. Koh and Y. Kwon, *J. Power Sources*, 2015, **286**, 197–203.
- 2 D. Ivnitski, K. Artyushkova, R. A. Rincon, P. Atanassov, H. R. Luckarift and G. R. Johnson, *Small*, 2008, **4**, 357–364.
- 3 A. Ramanavicius, A. Kausaite and A. Ramanaviciene, *Biosens. Bioelectron.*, 2008, **24**, 761–766.
- 4 L. Bahshi, M. Frascioni, R. Tel-Vered, O. Yehezkel, I. Willner, *Anal. Chem.*, 2008, **80**, 8253–8259.
- 5 R. Haddad, J.-G. Mattei, J. Thery and A. Auger, *Nanoscale*, 2015, **7**, 10641–10647.
- 6 S. B. Bankar, M. V. Blue, R. S. Singhal and L. Ananthanarayan, *Biotechnol. Adv.*, 2009, **27**, 489–501.

- 7 N. Mano, F. Mao and A. Heller, *J. Am. Chem. Soc.*, 2003, **125**, 6588–6594.
- 8 A. Ramanavicius, A. Kausaite and A. Ramanaviciene, *Biosens. Bioelectron.*, 2008, **24**, 761–766.
- 9 A. Guiseppi-Elie, C. Lei and R. H. Baughman, *Nanotechnology*, 2002, **13**, 559–564.
- 10 Y. Liu, M. Wang, F. Zhao, Z. Xu and S. Dong, *Biosens. Bioelectron.*, 2005, **21**, 984–8.
- 11 J. Hodak, Jose; Etchenique, Roberto; Calvo, Ernesto, *Langmuir*, 1997, **13**, 2708–2716.
- 12 R. Schoevaart, M. W. Wolbers, M. Golubovic, M. Ottens, a. P. G. Kieboom, F. Van Rantwijk, L. a M. Van Der Wielen and R. a. Sheldon, *Biotechnol. Bioeng.*, 2004, **87**, 754–762.
- 13 R. a. Sheldon, *Appl. Microbiol. Biotechnol.*, 2011, **92**, 467–477.
- 14 A. K. Boal, H. Tellez, S. Rivera, N. Miller, E. G. D. Bachand and B. C. Bunker, *Small*, 2006, **2**, 793–803
- 15 R. Bahulekar, N. R. Ayyangar, and S. Ponrathnam, 1991, *Enzyme Microb. Technol.*, 1991, **13**, 858–868.
- 16 M. P. Xiong, M. Laird Forrest, G. Ton, A. Zhao, N. M. Davies and G. S. Kwon, *Biomaterials*, 2007, **28**, 4889–4900.
- 17 K. H. Hyun, J. H. Lee, C. W. Yoon and Y. Kwon, *Int. J. Electrochem. Sci.*, 2013, **8**, 1752–11767.
- 18 K. H. Hyun, J. H. Lee, C. W. Yoon, Y. H. Cho, L. H. Kim and Y. Kwon, *Synth. Met.*, 2014, **190**, 48–55
- 19 M. Christwardana and Y. Kwon, *J. Power Sources*, 2015, **299**, 604–610.
- 20 Y. Liu, L. Liu and S. Dong, *Electroanalysis*, 2007, **19**, 55–59.
- 21 P. Kavanagh and D. Leech, *Phys. Chem. Chem. Phys.*, 2013, **15**, 4859–69.
- 22 S. Xu, H. Qi, S. Zhou, X. Zhang and C. Zhang, *Microchim. Acta*, 2014, **181**, 535–541.
- 23 J. H. Kim, H. J. Lee, H. Jung, H.-K. Song, H. H. Yoon and K. Won, *Mol. Cryst. Liq. Cryst.*, 2010, **519**, 82–89.
- 24 Y. Xiao, F. Patolsky, E. Katz, J. F. Hainfeld and I. Willner, *Science*, 2003, **299**, 1877–1881.
- 25 B. Kaczmarczyk, *J. Mol. Struct.*, 2013, **1048**, 179–184.
- 26 T. Kurihara, N. Oba, Y. Mori, S. Tomaru and T. Kaino, *J. Appl. Phys.*, 1991, **70**, 17–19.
- 27 A. Kumar, M. V. Rao and S. K. Menon, *Tetrahedron Lett.*, 2009, **50**, 6526–6530.
- 28 F. Wang, P. Liu, T. Nie, H. Wei and Z. Cui, *Int. J. Mol. Sci.*, 2013, **14**, 17–29.
- 29 J. Wang and Q. Liu, *Nanoscale*, 2014, **6**, 4148.
- 30 T. Kuila, A. K. Mishra, P. Khanra, N. H. Kim and J. H. Lee, *Nanoscale*, 2013, **5**, 52–71.
- 31 K. Murphy, W. Tysoe and D. Bennett, *Langmuir*, 2004, **20**, 1732–1738.
- 32 D. Ivnitski, B. Branch, P. Atanassov and C. Apblett, *Electrochem. Commun.*, 2006, **8**, 1204–1210.
- 33 S. Liu and H. Ju, *Biosens. Bioelectron.*, 2003, **3**, 177–183.
- 34 E. Laviron, *J. Electroanal. Chem.*, 1979, **101**, 19–28.
- 35 A. P. Periasamy, Y. J. Chang and S. M. Chen, *Bioelectrochemistry*, 2011, **80**, 114–120.
- 36 F. Gutierrez, M. D. Rubianes and G. A. Rivas, *Sensors Actuators B Chem.*, 2012, **161**, 191–197.
- 37 M. Wooten, S. Karra, M. Zhang and W. Gorski, *Anal. Chem.*, 2014, **86**, 752–757.
- 38 K. H. Hyun, S. W. Han, W.-G. Koh and Y. Kwon, *Int. J. Hydrogen Energy*, 2015, **2**, 2199–2206.
- 39 S. Zhang, N. Wang, H. Yu, Y. Niu and C. Sun, *Bioelectrochemistry*, 2005, **67**, 15–22.
- 40 R. A. Kamin and G. S. Wilson, *Anal. Chem.*, 1980, **52**, 1198–1205.
- 41 B. M. Fischback, J. K. Youn, X. Y. Zhao, P. Wang, H. G. Park, H. N. Chang, J. Kim and S. Ha, *Electroanalysis*, 2006, **18**, 2016–2022.
- 42 J. Sun, H. Zhao, Q. Yang, J. Song and A. Xue, *Electrochimica Acta*, 2010, **55**, 3041–3047.